AIP | Journal of Applied Physics

Low temperature structural variations of Na0.5Bi0.5TiO3-7%BaTiO3 single crystal: Evidences from optical ellipsometry and Raman scattering

T. Huang, S. Guo, L. P. Xu, C. Chen, Z. G. Hu, H. S. Luo, and J. H. Chu

Citation: Journal of Applied Physics **117**, 224103 (2015); doi: 10.1063/1.4922424
View online: http://dx.doi.org/10.1063/1.4922424
View Table of Contents: http://scitation.aip.org/content/aip/journal/jap/117/22?ver=pdfcov
Published by the AIP Publishing

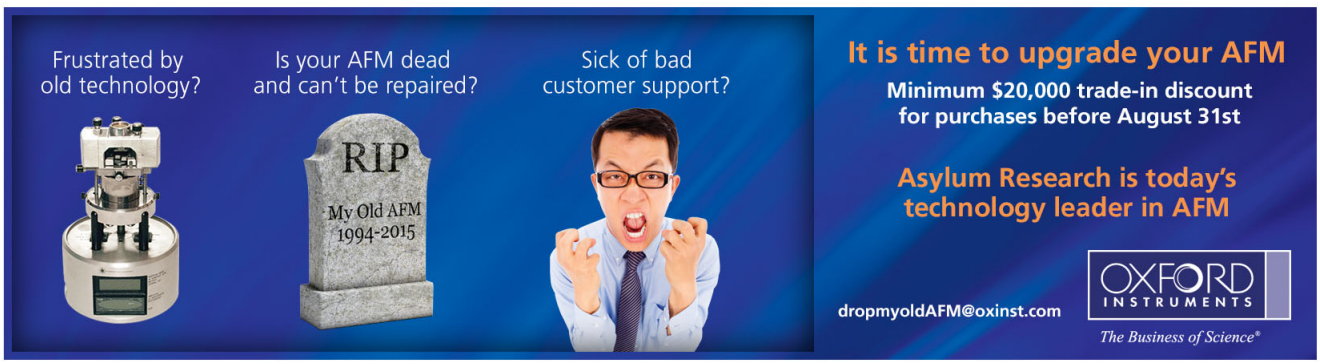

Low temperature structural variations of $Na_{0.5}Bi_{0.5}TiO_3$-7%$BaTiO_3$ single crystal: Evidences from optical ellipsometry and Raman scattering

T. Huang,[1] S. Guo,[1] L. P. Xu,[1] C. Chen,[2] Z. G. Hu (胡志高),[1,a)] H. S. Luo,[2] and J. H. Chu[1]
[1]*Key Laboratory of Polar Materials and Devices, Ministry of Education, Department of Electronic Engineering, East China Normal University, Shanghai 200241, China*
[2]*Key Laboratory of Inorganic Functional Materials and Devices, Shanghai Institute of Ceramics, Chinese Academy of Sciences, Shanghai 201800, China*

(Received 17 March 2015; accepted 1 June 2015; published online 11 June 2015)

Optical properties and structural variations of $Na_{0.5}Bi_{0.5}TiO_3$-7%$BaTiO_3$ (NBT-7%BT) single crystal have been studied by temperature-dependent optical ellipsometry and Raman spectroscopy from 4.2 to 300 K. The second derivative of the complex dielectric functions reveals two interband transitions (E_{cp1} and E_{cp2}) located at about 3.49 and 4.25 eV, respectively. Depending on the temperature evolution of electronic transitions, structural variations appear near 60, 150, and 240 K, respectively. These anomalies are also well illustrated from the low-frequency phonon modes involving vibrations of Bi. The low-temperature structural variations of NBT-7%BT crystal can be associated with instability of the crystalline lattice driven by off-centered Bi ions, followed by the variations of polarizability of the unit cells. © *2015 AIP Publishing LLC*.
[http://dx.doi.org/10.1063/1.4922424]

I. INTRODUCTION

Recently, there is an increasing emphasis on lead-free ferroelectric morphotropic phase boundary (MPB) systems, for the reason that systems with MPB between different competing phases are correlated with enhanced piezoelectric properties. $Na_{0.5}Bi_{0.5}TiO_3$ (NBT) and NBT-based compounds, which exhibit relatively large spontaneous polarization and high Curie temperature, have gained considerable attention as lead-free candidates to replace nowadays widely used lead zirconate titanate based piezoelectric materials from the view point of environmental protection.[1] Among NBT-based solid solutions, $Na_{0.5}Bi_{0.5}TiO_3$-x%$BaTiO_3$ (NBT-x%BT) has a MPB between rhombohedral and tetragonal phases in the region of $6 < x < 8$.[1] Generally, the studies in regard to changes of NBT-x%BT ($6 < x < 8$) structure mainly focus on temperature interval above room temperature (RT).[2–5] However, previous studies have suggested the structural changes of NBT-based systems below RT. Suchanicz *et al*. have reported a phase transition of NBT single crystal at 55 K, merged as a small anomaly in the elastic stiffness moduli, phonon mean free path and dielectric losses experiments.[6] Also, depending on low-temperature neutron powder diffraction, it revealed a slight anomaly in the lattice parameters in the vicinity of 55 K.[7] In addition, anomalous behavior was found in the generalized density of states from NBT near 120 K.[8] Therefore, one may suggest that phase transition process of NBT-x%BT system below RT is far away from the clarification. As we know, the phase transition is intrinsically related to the crystalline structure variation, which can result in different optical response behaviors.[9–11] What's more, physical properties of NBT-x%BT material, such as electrical and optical characteristics, should be thoroughly studied for the potential applications in optoelectronics.[12] On this occasion, further investigations especially optical properties are necessary. Furthermore, the thermal broadening of optical transitions is reduced and individual optical structures are better decomposed at low temperature.[9] That is to say, the optical information of materials at low temperature plays a significant role in comprehending the electronic structure of studied ones. As a result, it is significative to explore the optical properties of NBT-x%BT at low temperature.

Optical ellipsometry is regarded as a highly appropriate technique to determine the optical constants of specimen such as complex dielectric function $\varepsilon = \varepsilon_1 + i\varepsilon_2$ over a wide spectral range.[9] What's more, interband critical points (CPs), which are obtained from optical ellipsometry data, have shown efficiency in exploring phase transition of many semiconductor and dielectric materials, as well as ferroelectrics.[9–11] Likewise, nondestructive Raman scattering that provides precise information about ionic configurations and local distortions in the crystal structures has been widely used for studying phase transitions in ferroelectrics, including NBT and NBT-based systems.[3,13–17] Therefore, combined optical and phonon spectroscopy can be a valid methodology to explore the phase transition of NBT-7%BT below RT.

In this article, the interband transitions and phonon modes of $Na_{0.5}Bi_{0.5}TiO_3$-7%$BaTiO_3$ (NBT-7%BT) crystal have been investigated by optical ellipsometry and Raman spectra as a function of temperature from 4.2 to 300 K, respectively. The physical mechanism related to the structural variation pattern of NBT-7%BT crystal has been discussed in detail.

II. EXPERIMENTAL DETAILS

NBT-7%BT single crystals were grown by a top-seeded solution growth method. The raw materials were high-purity

a)Author to whom correspondence should be addressed. Electronic mail: zghu@ee.ecnu.edu.cn. Tel.: +86-21-54345150. Fax: +86-21-54345119.

(99.99%) powders of Na_2CO_3, Bi_2O_3, Ba_2CO_3, and TiO_2. The NBT and $BaTiO_3$ (BT) powders with stoichiometric ratio were mixed completely, and then placed in a muffle furnace for solid-state reaction. The solid-state reaction temperatures of NBT and BT are determined to be about 860 and 1160 °C, respectively. The single crystals were grown in a Pt crucible, which was heated by using a resistance furnace in an air atmosphere. Small $(001)_{PC}$ oriented crystals were used as the seeds for crystal growth, and the velocities of rotation and pulling of the seed were in the ranges of 6–12 rpm and 1.2–2.5 mm per day, respectively. At the end of crystal growth, the crystal was separated from the flux-melt surface and cooled down at a rate of 50–60 °C/h to room temperature. The obtained NBT-7%BT single crystals were cut into a $10 \times 10 \times 0.3\,mm^3$ size parallel the $(001)_{PC}$ face with single-side polished.[4] The X-ray powder diffraction results indicate that NBT-7%BT single crystals are at MPB between rhombohedral and tetragonal phases at room temperature.[4] Note that the specimen has been annealed (~400 °C) after the mechanical polishing, then cleaned in pure ethanol with an ultrasonic bath and rinsed by deionized water for several times prior to spectral measurements. The root-mean-square roughness was estimated to be about 5 nm by atomic force microscopy (AFM, Digital Instruments Dimension Icon, Bruker). Temperature-dependent optical ellipsometry experiments were performed by a vertical variable-angle nearinfrared-ultraviolet optical ellipsometry (J. A. Woollam Co., Inc.) for the photon energy region from 1.12 to 6.2 eV (200–1100 nm) with an incident angle of 70°. The spectral resolution of optical ellipsometry is set to 5 nm, and the measurements were carried out with auto retarder (high accuracy). The sample was mounted into Janis CRV-217 V with liquid helium as cooling accessories for low temperature experiments. Note that the window corrections were included as a part of the model used for analysis and all the fitting procedure was completed through WVASE32 software package (J. A. Woollam Co., Inc.). Temperature-dependent Raman scattering measurements were carried out by a Jobin-Yvon LabRAM HR 800 UV micro-Raman spectrometer and a heating/cooling stage (Microstat HiRes, Oxford). A laser with the wavelength of 632.8 nm was used as the excitation source and an air-cooled charge coupled device (CCD) was used to collect the scattered signal dispersed on 1800 grooves/mm grating in the frequency range of 10–1000 cm^{-1}, with the use of ultra low frequency (ULF) filter. The spectral resolution of Raman spectra is better than 0.65 cm^{-1}. For both optical ellipsometry and Raman experiments, the temperature was varied from 4.2 to 300 K with a resolution of 1 K.

III. RESULTS AND DISCUSSION

For the purpose of estimating the roughness of the crystal more accurate, a three-layer model (air/surface roughness/crystal) was applied in this study. The surface roughness layer was modeled by Brüggeman effective-medium approximation; the complex dielectric function of NBT-7%BT crystal was estimated from parametric oscillators Psemi-M0 and Psemi-M3.[10] The model is in good agreement with Ψ and Δ measured at different incident angles (50°, 60°, and 70°), as revealed in Figs. 1(a) and 1(b), respectively. Therefore, it is proved that the fitted thickness of the roughness layer (4.5 nm) is credible, which agrees with the root-mean-square value (5 nm) of NBT-7%BT single crystal measured by AFM. Given the accurate thickness of the roughness layer, numerically inverted complex dielectric function (NICDF) of NBT-7%BT crystal at every temperature was directly calculated from the original experimental data, which is believed to be more scientifically rigorous than the complex dielectric function as revealed in recent studies.[10] Fig. 1(c) illustrates the NICDF at 4.2 and 300 K. It can be seen that the imaginary part ε_2 at 300 K is almost equal to zero below 3.4 eV (near the absorption edge) then increases sharply with increasing photon energy due to a strong optical absorption. The ε_1 and ε_2 exhibit strong dispersion relation with increasing photon energy. The dispersion behaviors have been observed in most ABO_3-type perovskite structure compounds.[10,11,18] As for NBT-7%BT crystal, the basic BO_6 (TiO_6) octahedron building block determines low-lying conduction bands together with the highest valence bands, due to the association of B-site *d* orbits with the O-2*p* ones.[18] The lowest energy oscillator plays a significant role in the dispersion optical behavior and leads to similar energy band structure of NBT-7%BT crystal with other ABO_3 type compounds.

To analyze the temperature evolution of interband transitions, the CP energies were obtained by fitting the second derivative of NICDF.[10] In this work, a total of two excitonic line shapes were used to fit the data from 2 to 6.2 eV. Note that the real and imaginary parts were fitted simultaneously. The $d^2\varepsilon_1/dE^2$ and $d^2\varepsilon_2/dE^2$ spectra calculated from the experimental data, and the corresponding best-fitted curves at 300 K are shown in Fig. 1(d). It indicates that two distinct transitions can be readily distinguished. For clarity, a set of

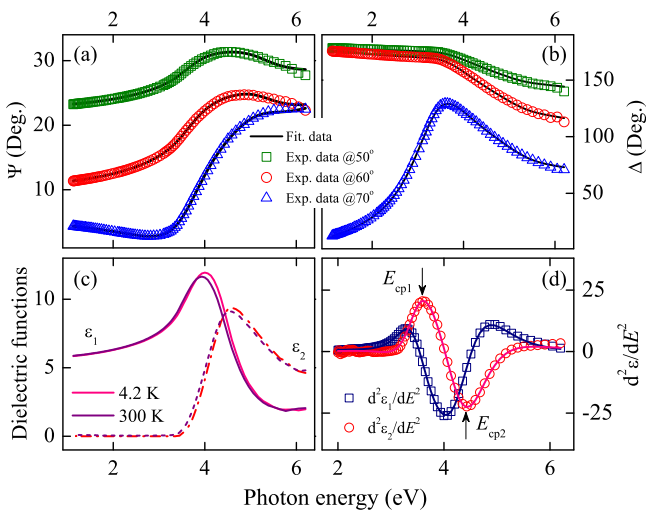

FIG. 1. The experimental data (dots) and calculation curves (lines) of (a) Ψ and (b) Δ recorded with various incident angle at 50°, 60°, and 70°. (c) The real part and imaginary part of numerically inverted complex dielectric functions at 4.2 and 300 K, which are directly calculated from the original spectra by taking the thickness of roughness layer into account. (d) The second derivative of the complex dielectric functions spectra (dots) and the best-fit curves (lines) at 300 K. Note that the CPs positions are marked with arrows.

TABLE I. The best-fitting parameters of SCP model for NBT-7%BT single crystal extracted from the second derivative of NICDF at specific temperatures.

	E_1				E_2			
Temperature (K)	A_1	ϕ_1 (eV)	E_{cp1} (eV)	Γ_1 (deg.)	A_2	ϕ_2 (eV)	E_{cp2} (eV)	Γ_2 (deg.)
4.2	1.53	43.5	3.58	0.64	9.49	40.1	4.33	0.92
110	1.45	43.4	3.56	0.65	9.65	40.1	4.30	0.92
200	1.35	43.4	3.54	0.63	9.39	40.1	4.29	0.93
300	1.33	43.3	3.49	0.64	9.86	40.0	4.25	0.95

the fitting parameters at specific temperatures is listed in Table I. The physical origin of two CPs can be illustrated in the light of electronic band structures. According to the first-principles calculations, the electronic band structure of NBT-7%BT to some extent is similar to that of NBT.[19] As for rhombohedral phase of NBT at RT, the top of the valence band (VB) (at the Γ point) is primarily constituted of O-2*p* states, whereas the bottom of the conduction band (CB) (at the Γ point) arises mainly from Ti-3*d* and Bi-6*p* states.[12,17] Therefore, the first CP of NBT-7%BT at 3.49 eV corresponds mainly to the transitions from the O-2*p* VB to Ti-3*d* or Bi-6*p* lower-energy CB. However, the second one at 4.25 eV is due to the transition from O-2*p* VB to Ti-3*d* or Bi-6*p* high-energy CB.

Figs. 2(a) and 2(b) indicate that both the CP energies in general show a red shift upon heating, which is due to the electron-phonon interaction and the lattice thermal expansion.[20] When temperature increases, the interatomic distance along the direction of their propagation can be altered by the longitudinal phonons,[21] which can finally move the CB downward and the VB upward. According to the slope changes of the dependencies for CP energies, the variation of both E_{cp1} and E_{cp2} can be separated into four parts: Part (i) to Part (iv). To better illustrate the various trends of the two CPs, every region was linearly fitted. As can been seen from Figs. 2(a) and 2(b), interrupts of slope for E_{cp1} and E_{cp2} variation take place near 60, 150, and 240 K, which can give evidence for structural variations in NBT-7%BT crystal at low temperature.

To confirm whether the structural changes of NBT-7% BT crystal appear at low-temperature, Raman spectra were collected from 4.2 to 300 K on heating. To eliminate the effect of temperature on the peak intensities, Bose-Einstein population factor are applied to correct the spectra. It should be noted that the temperature dependence remaining after Bose-Einstein correction can only results from dynamical changes in the internal state of crystal system.[13] Fig. 3(a) shows temperature-dependent Raman spectra of NBT-7% BT, as well as the Lorentzian-shaped deconvolution at 4.2 K, which illustrates that low-frequency part consists of two phonon modes near 30 and 54 cm^{-1}. The Raman spectra of NBT-7%BT crystal at ambient conditions can be mainly divided into three parts. In NBT-based solid solutions, the Raman peak near 54 cm^{-1} should be dominated by Bi vibrations,[22] which reflects the coupling processes within the subsystem of off-centered Bi.[13,14] Recently, the importance of Bi has been shown in various Bi-based ferroelectrics, including the model multiferroic $BiFeO_3$.[22–24] Moreover, the lone-pair electrons of Bi has been proposed to play an important role in NBT-based solid solutions.[13,14,23] Therefore, special attention has been paid to the vibrations of Bi in this work, i. e., the low-frequency part of the spectrum below 100 cm^{-1}. As for the mode near 120 cm^{-1}, it was previously ascribed to the vibrations of A-site Na cation,[16] but recently is believed to be dominated by Bi-TiO_3 vibrations.[13] The scattering near

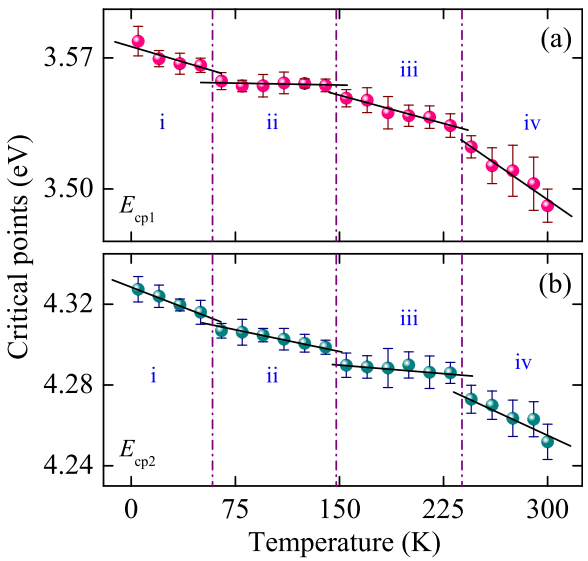

FIG. 2. Temperature dependence of two critical-point energies for (a) E_{cp1} and (b) E_{cp2} with linearly fitting results (solid lines). The dash-dot lines are applied to guide the eyes and indicate anomaly behavior.

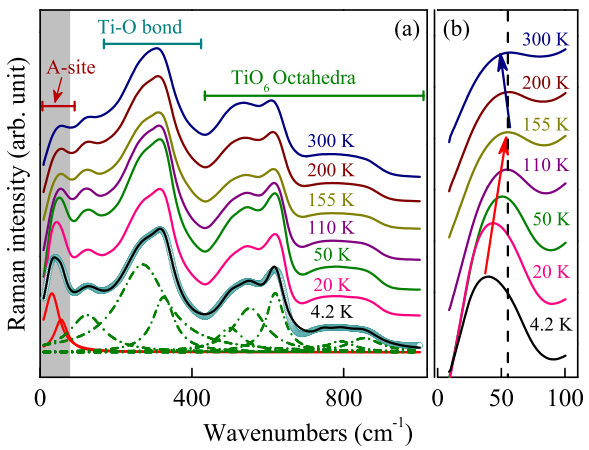

FIG. 3. (a) Raman spectra of NBT-7%BT, corrected by Bose-Einstein population factor, as a function of temperature from 4.2 to 300 K, with the Lorentzian-shaped spectral deconvolution at 4.2 K. The assignment of the spectral modes to particular lattice vibrations is also indicated. (b) The enlarged part of low-frequency region below 100 cm^{-1} [grey part in (a)]. Note that the arrows illustrate the evolution trend of phonon frequency.

290 cm^{-1} and the high-frequency bands above 450 cm^{-1} should involve vibrations of Ti-O bond and TiO_6 octahedra, respectively.[14,16] From Fig. 3(a), the whole spectrum undergoes broadening with increasing temperature. As for the low-frequency part, it is easily distinguished from the high-frequency ones, and becomes a shoulder at low-temperature 4.2 K. Take a further observation, low-frequency part first undergoes apparent increasing, till 150 K approximately; then slightly decreasing to 300 K, as can be clearly seen in Fig. 3(b).

Fig. 4 illustrates the frequency and full width at half maximum (FWHM) of the modes (near 30 and 54 cm^{-1}) related to Bi vibrations with increasing temperature, respectively. In the phonon frequency of the Bi vibrations [Figs. 4(a) and 4(b)], three anomalies are represented near 60, 150, and 240 K, respectively. The frequency of two modes increases constantly from 4.2 to 150 K then stars to decrease gradually till 300 K. The three anomalies are also reflected from the FWHM [Figs. 4(c) and 4(d)] of Bi vibrations. However, FWHM values of the modes near 30 and 54 cm^{-1} above 240 K exhibit decreasing and increasing trend, respectively. The visible anomalies near 60, 150, and 240 K in both frequency and FWHM of Bi vibrations, where the discontinuities occur, can be related to structural variations.

Based on the aforementioned discussion, the structural variations of NBT-7%BT crystal at low temperature can be well illustrated from both optical ellipsometry and low-frequency Raman scattering at about 60, 150, and 240 K, which rely on the temperature evolutions of the CP energies (Fig. 2) as well as frequency and FWHM of Bi vibrations (Fig. 4), respectively. It is noteworthy that all the Raman spectra have been corrected by the Bose-Einstein temperature factor to facilitate comparison and eliminate the contribution from the Bose-Einstein population factor. And, the normalization of the Raman spectra to the Bose-Einstein occupation factor does not influence the frequency and full width at half maximum (FWHM). It seems that structure variations of NBT-7%BT at low temperature are associated with off-centered Bi ions. In fact, even in the ideal cubic structure, where Ti is in the center of oxygen octahedra and Na or Bi is in the center of oxygen cuboctahedra, Bi ion tends to exhibit the off-center site to hybridize with the O ion. In the case of the rhombohedral phase at low temperature, Bi has the largest off-centering from the center of the O cages, owing to its stereochemical activity and large volume in A-site created by larger radius of Na.[25] Note that Bi vibrations affect distances of the bonding between the Bi and oxygen ions. As for the Raman data, the frequency of the Bi vibrations increases till 150 K can indicate a strengthening of the bonding between the Bi and oxygen ions. However, the frequency decreases above 150 K can indicate a weakening of the bonding between the Bi and oxygen ions, and can be related to the loss of orbital hybridization between the Bi-6*p* and O-2*p* orbitals.[14] Since hybridization of Bi-6*p* and O-2*p* increases the stability of structures with layers of high Bi-concentrations in {001}-planes,[24] it can imply that a more disordered lattice is obtained above 150 K. In addition, the FWHM signifies the degree of disorder in the lattice.[8] As a consequence, the FWHM of Bi vibrations decrease below 60 K can imply the lattice exhibits distortion toward ordered, while FWHM increase from 150 to 240 K suggest the change from ordered to distortion. As for different trends of FWHM for 30 and 54 cm^{-1} above 240 K, it may be related to predominantly rhombohedrally off-centered Bi^{3+} cations form two different polar displacements.[23] In this work, the off-centering of Bi (A-site) can interpret the variation of E_{cp1} and E_{cp2}, which are assigned as the transitions from the O-2*p* VB to Ti-3*d* or Bi-6*p* lower-energy and high-energy CB, respectively. Raman data can indicate that the Bi off-centering is followed by the variations of polarizability of the unit cells, which results from the change in the bond situation of Bi and oxygen ions from strengthening to weakening. Part (i) and Part (iv) of E_{cp1} and E_{cp2} correspond to the relative large and small polarizability of the unit cells, respectively. Therefore, the structure variations of NBT-7% BT crystal below 300 K could result from the instability of crystalline lattice driven by off-centered Bi ions. However, the mechanics of the low-temperature optical anomalies of NBT-7%BT near 60, 150, and 240 K need further study.

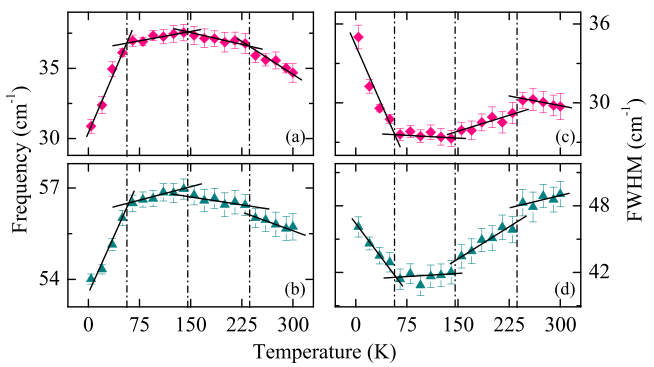

FIG. 4. (a) and (b) The frequency of the two modes near 30 and 54 cm^{-1} as a function of temperature, respectively. (c) and (d) Full width at half maximum (FWHM) of these two modes. Keep in mind that the dashed lines indicate the locations of the abnormal points (near 60, 150, and 240 K).

IV. SUMMARY

In conclusion, temperature-dependent optical ellipsometry and Raman spectra of NBT-7%BT single crystal have been investigated at low temperature down to 4.2 K. It reveals structural variations occur near 60, 150, and 240 K, depending on the evolutions of critical point energies obtained by fitting the second derivative of numerically inverted complex dielectric functions. These variations are verified in low-frequency Raman scattering involving Bi vibrations. The structure variations of NBT-7% below 300 K could be the consequence of instability of the crystalline lattice driven by off-centered Bi ions and the mechanics of the low-temperature optical anomalies of NBT-7%BT near 60, 150, and 240 K need further study.

ACKNOWLEDGMENTS

One of the authors (T.H.) would like to thank Dr. Jinzhong Zhang and Dr. Jiajun Zhu for fruitful discussions. This work was financially supported by Major State Basic

Research Development Program of China (Grant Nos. 2011CB922200 and 2013CB922300), Natural Science Foundation of China (Grant Nos. 11374097 and 61376129), Projects of Science and Technology Commission of Shanghai Municipality (Grant Nos. 14XD1401500, 13JC1402100, and 13JC1404200), and the Program for Professor of Special Appointment (Eastern Scholar) at Shanghai Institutions of Higher Learning.

[1]T. Takenaka, K. Maruyama, and K. Sakata, Jpn. J. Appl. Phys. **30**, 2236 (1991).
[2]W. W. Ge, D. Maurya, J. F. Li, S. Priya, and D. Viehland, Appl. Phys. Lett. **102**, 222905 (2013).
[3]T. Huang, Z. G. Hu, G. S. Xu, X. L. Zhang, J. Z. Zhang, and J. H. Chu, Appl. Phys. Lett. **104**, 111908 (2014).
[4]Q. H. Zhang, X. Y. Zhao, R. B. Sun, and H. S. Luo, Phys. Status Solidi A **208**, 1012 (2011).
[5]C. Ma, X. Tan, E. Dul'kin, and M. Roth, J. Appl. Phys. **108**, 104105 (2010).
[6]J. Suchanicz, A. Jeżowski, and R. Poprawski, Phys. Status Solidi A **169**, 209 (1998).
[7]G. O. Jones and P. A. Thomas, Acta Crystallogr., Sect. B: Struct. Sci. **58**, 168 (2002).
[8]S. G. Lushnikov, S. N. Gvasaliya, I. G. Siny, I. L. Sashin, V. H. Schmidtc, and Y. Uesu, Solid State Commun. **116**, 41 (2000).
[9]S. G. Choi, R. Chen, C. Persson, T. J. Kim, S. Y. Hwang, Y. D. Kim, and L. M. Mansfield, Appl. Phys. Lett. **101**, 261903 (2012).
[10]X. Chen, P. P. Jiang, Z. H. Duan, Z. G. Hu, X. F. Chen, G. S. Wang, X. L. Dong, and J. H. Chu, Appl. Phys. Lett. **103**, 192910 (2013).
[11]S. Zhang, J. Z. Zhang, M. J. Han, Y. W. Li, Z. G. Hu, and J. H. Chu, Appl. Phys. Lett. **104**, 041106 (2014).
[12]M. Zeng, S. W. Or, and H. L. W. Chan, J. Appl. Phys. **107**, 043513 (2010).
[13]K. Datta, A. Richter, M. Göbbels, R. B. Neder, and B. Mihailova, Phys. Rev. B **90**, 064112 (2014).
[14]D. Schütz, M. Deluca, W. Krauss, A. Feteira, T. Jackson, and K. Reichmann, Adv. Funct. Mater. **22**, 2285 (2012).
[15]J. Petzelt, S. Kamba, J. Fábry, D. Noujni, V. Porokhonskyy, A. Pashkin, I. Franke, K. Roleder, J. Suchanicz, R. Klein, and G. E. Kugel, J. Phys.: Condens. Matter **16**, 2719 (2004).
[16]J. Kreisel, A. M. Glazer, G. Jones, P. A. Thomas, L. Abello, and G. Lucazeau, J. Phys.: Condens. Matter **12**, 3267 (2000).
[17]M. K. Niranjan, T. Karthik, S. Asthana, J. Pan, and U. V. Waghmare, J. Appl. Phys. **113**, 194106 (2013).
[18]M. Otonicar, S. D. Skapin, M. Spreitzer, and D. Suvorov, J. Eur. Ceram. Soc. **30**, 971 (2010).
[19]Y.-N. Xu and W. Y. Ching, Philos. Mag. B **80**, 1141 (2000).
[20]S. A. Lourenco, I. F. L. Dias, J. L. Duarte, E. Laureto, E. A. Meneses, J. R. Leite, and I. Mazzaro, J. Appl. Phys. **89**, 6159 (2001).
[21]S. Biernacki, U. Scherz, and B. K. Meyer, Phys. Rev. B **49**, 4501 (1994).
[22]V. N. Denisov, A. N. Ivlev, A. S. Lipin, B. N. Mavrin, and V. G. Orlov, J. Phys.: Condens. Matter **9**, 4967 (1997).
[23]D. S. Keeble, E. R. Barney, D. A. Keen, M. G. Tucker, J. Kreisel, and P. A. Thomas, Adv. Funct. Mater. **23**, 185 (2013).
[24]M. Gröting, S. Hayn, and K. Albe, J. Solid State Chem. **184**, 2041 (2011).
[25]H. F. Lü, S. Y. Wang, and X. S. Wang, J. Appl. Phys. **115**, 124107 (2014).